
TEMPORAL DOMAIN GENERALIZATION WITH DRIFT-AWARE DYNAMIC NEURAL NETWORK

Guangji Bai*

Department of Computer Science
Emory University
Atlanta, GA
guangji.bai@emory.edu

Chen Ling*

Department of Computer Science
Emory University
Atlanta, GA
chen.ling@emory.edu

Liang Zhao†

Department of Computer Science
Emory University
Atlanta, GA
liang.zhao@emory.edu

May 24, 2022

ABSTRACT

Temporal domain generalization is a promising yet extremely challenging area where the goal is to learn models under temporally changing data distributions and generalize to unseen data distributions following the trends of the change. The advancement of this area is challenged by: 1) characterizing data distribution drift and its impacts on models, 2) expressiveness in tracking the model dynamics, and 3) theoretical guarantee on the performance. To address them, we propose a Temporal Domain Generalization with Drift-Aware Dynamic Neural Network (DRAIN) framework. Specifically, we formulate the problem into a Bayesian framework that jointly models the relation between data and model dynamics. We then build a recurrent graph generation scenario to characterize the dynamic graph-structured neural networks learned across different time points. It captures the temporal drift of model parameters and data distributions and can predict models in the future without the presence of future data. In addition, we explore theoretical guarantees of the model performance under the challenging temporal DG setting and provide theoretical analysis, including uncertainty and generalization error. Finally, extensive experiments on several real-world benchmarks with temporal drift demonstrate the proposed method’s effectiveness and efficiency.

1 Introduction

In machine learning, researchers often assume that training and test data follow the same distribution for the trained model to work on test data with some generalizability. However, in reality, this assumption usually cannot be satisfied, and when we cannot make sure the trained model is always applied in the same domain where it was trained. This motivates Domain Adaptation (DA) which builds the bridge between source and target domains by characterizing the transformation between the data from these domains [1, 2, 3]. However, in more challenging situations when target domain data is unavailable (e.g., no data from an unknown area, no data from the future, etc.), we need a more realistic scenario named Domain Generalization (DG) [4, 5, 6].

Most existing works in DG focus on generalization among domains with categorical indices, such as generalizing the trained model from one dataset (e.g., MNIST [7]) to another (e.g., SVHN [8]), from one task (e.g., image classification [9]) to another (e.g., image segmentation [10]), etc. However, in many real-world applications, the “boundary” among different domains is unavailable and difficult to detect, leading to a *concept drift* across the domains. For example, when a bank leverages a model to predict whether a person will be a “defaulted borrower”, features like “annual incoming”, “profession type”, and “marital status” are considered. However, due to the temporal change of the society, how these feature values indicate the prediction output should change accordingly following some trends that could be predicted somehow in a range of time. Figure 1 shows another example, seasonal flu prediction via Twitter data which evolves each year in many aspects. For example, monthly active users are increasing, new friendships are formed, the age distribution is shifting under some trends, etc. Such temporal change in data distribution gradually outdated the

*Equal contribution.

†Corresponding author.

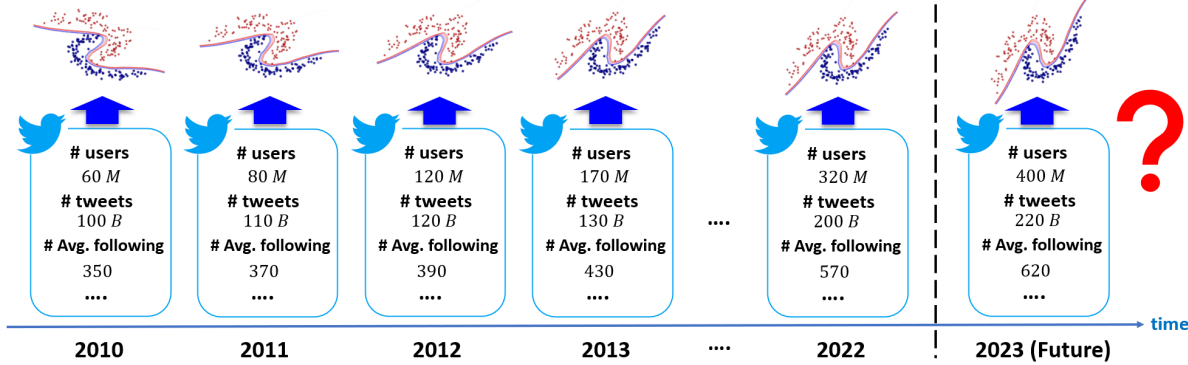


Figure 1: **An illustrative example of temporal domain generalization.** Consider training a machine learning model for some classification tasks based on the annual Twitter dataset such that the trained model can generalize to the future domains (e.g., 2023). The temporal drift of data distribution can influence the prediction model such as the rotation of the decision boundary in this case.

models. Correspondingly, suppose there was an ideal, always update-to-date model, then the model parameters should gradually change correspondingly to counter the trend of data distribution shifting across time. It can also “predict” what the model parameters should look like in an arbitrary (not too far) future time point. This requires the power of *temporal* domain generalization.

However, as an extension of traditional DG, temporal DG is extremely challenging yet promising. Existing DG methods that treat the domain indices as a categorical variable may not be suitable for temporal DG as they require the domain boundary as *a priori* to learn the mapping from source to target domains [11, 12, 13, 5]. Until now, temporal domain indices have been well explored only in DA [14, 15, 16] but not DG. There are very few existing works in temporal DG due to its big challenges. One relevant work is *Sequential Learning Domain Generalization* (S-MLDG) [17] that proposed a DG framework over sequential domains via meta-learning [18]. S-MLDG meta-trains the target model on all possible permutations of source domains, with one source domain left for meta-test. However, S-MLDG in fact still treats domain index as a categorical variable, and the method was only tested on categorical DG dataset. A more recent paper called *Gradient Interpolation* (GI) [19] proposes a temporal DG algorithm to encourage a model to learn functions that can extrapolate to the near future by supervising the first-order Taylor expansion of the learned function. However, GI has very limited power in characterizing model dynamics because it can only learn how the activation function changes along time while making all the remaining parameters fixed across time.

The advancement of temporal domain generalization is challenged by several critical bottlenecks, including **1) Difficulty in characterizing the data distribution drift and its influences on models.** Modeling the temporally evolving distributions requires making the model time-sensitive. Intuitive ways include feeding the time as an input feature to the model, which is well deemed simple yet problematic as it discards the other features’ dependency on time and dependency on other *confounding* factors changed along time [16]. Another possible way is to make the model parameters a function of time. However, these ways cannot generalize the model to future data as long as the whole model’s dynamics and data dynamics are not holistically modeled. **2) Lack of expressiveness in tracking the model dynamics.** Nowadays, complex tasks have witnessed the success of big complex models (e.g., large convolutional neural networks [20]), where the neurons and model parameters are connected as a complex graph structure. However, they also significantly challenge tracking their model dynamics in temporal DG. An expressive model dynamics characterization and prediction requires mapping data dynamics to *model dynamics* and hence the graph dynamics of model parameters across time. This is a highly open problem, especially for the temporal DG area. **3) Difficulty in theoretical guarantee on the performance.** While there are fruitful theoretical analyses on machine learning problems with independent-and-identically-distributed (*i.i.d*) assumptions (e.g., generalization error bound [21]), similar analyses meet substantial hurdles to be extended to out-of-distribution (*OOD*) problem due to the distribution drift over temporally evolving domains. Therefore, it is essential to enhance the theoretical analyses on the model capacity and theoretical relation among different temporal domain generalization models.

To address all the above challenges, we propose a Temporal Domain Generalization with DRift-Aware dynamIc neural Network (DRAIN) framework that solves all challenges above simultaneously in an end-to-end manner. Specifically, we propose a generic framework to formulate temporal domain generalization by a Bayesian treatment that jointly models the relation between data and model dynamics. To instantiate the Bayesian framework, a recurrent graph generation scenario is established to encode and decode the dynamic graph-structured neural networks learned across different

timestamps. Such a scenario can achieve a fully time-sensitive model and can be trained in an end-to-end manner. It captures the temporal drift of model parameters and data distributions, and can predict the models in the future *without* the presence of future data.

Our contributions include: **1)** We develop a novel and adaptive temporal domain generalization framework that can be trained in an end-to-end manner. **2)** We innovatively treat the model as a dynamic graph and leverage graph generation techniques to achieve a fully time-sensitive model. **3)** We propose to use the sequential model to learn the temporal drift adaptively and leverage the learned sequential pattern to predict the model status on the future domain. **4)** We provide theoretical analysis on both uncertainty quantification and generalization error of the proposed method. **5)** We demonstrate our model’s efficacy and superiority with extensive experiments.

2 Related work

Continuous Domain Adaptation. Domain Adaptation (DA) has received great attention from researchers in the past decade [1, 2, 3] and readers may refer to [22] for a comprehensive survey. Under the big umbrella of DA, continuous domain adaptation considers the problem of adapting to target domains where the domain index is a continuous variable (temporal DA is a special case when the domain index is 1D). Approaches to tackling such problems can be broadly classified into three categories: (1) biasing the training loss towards future data via transportation of past data[14, 15], (2) using time-sensitive network parameters and explicitly controlling their evolution along time [23, 24, 25], (3) learning representations that are time-invariant using adversarial methods [16]. The first category augments the training data, the second category reparameterizes the model, and the third category redesigns the training objective. However, data may not be available for the target domain, or it may not be possible to adapt the base model, thus requiring Domain Generalization.

Domain Generalization (DG). A diversity of DG methods have been proposed in recent years [11, 12, 26, 13, 5, 6, 19]. According to [27], existing DG methods can be categorized into the following three groups, namely: (1) *Data manipulation*: This category of methods focuses on manipulating the inputs to assist in learning general representations. There are two kinds of popular techniques along this line: a). Data augmentation [28, 29], which is mainly based on augmentation, randomization, and transformation of input data; b). Data generation [30, 31], which generates diverse samples to help generalization. (2) *Representation learning*: This category of methods is the most popular in domain generalization. There are two representative techniques: a). Domain-invariant representation learning [2, 32], which performs kernel, adversarial training, explicitly features alignment between domains, or invariant risk minimization to learn domain-invariant representations; b). Feature disentanglement [33], which tries to disentangle the features into domain-shared or domain-specific parts for better generalization. (3) *Learning strategy*: This category of methods focuses on exploiting the general learning strategy to promote the generalization capability, e.g, ensemble learning [34], meta-learning [6], gradient operation [35], etc.

Existing work above considers generalization across categorical domains, while in this paper, we assume the domain index set is across time (namely, temporal), and the domain shifts smoothly over time. Unfortunately, there is only very little work under this setting. The first work called *Sequential Learning Domain Generalization* (S-MLDG) [17] proposed a DG framework over sequential domains based on the idea of meta-learning. A more recent work called *Gradient Interpolation* (GI) [19] proposes a temporal DG algorithm to encourage a model to learn functions that can extrapolate well to the near future by supervising the first-order Taylor expansion of the learned function. However, neither work can adaptively learn the temporal drift across the domains while keeping the strong expressiveness of the learned model.

3 Methodology

In this section, we first provide the problem formulation of temporal domain generalization and then introduce our proposed framework, followed by our theoretical analyses of the proposed method.

3.1 Problem formulation

Temporal Domain Generalization. We consider prediction tasks where the data distribution evolves with time. During training, we are given T observed source domains $\mathcal{D}_1, \mathcal{D}_2, \dots, \mathcal{D}_T$ sampled from distributions on T arbitrary time points $t_1 \leq t_2 \leq \dots \leq t_T$, with each $\mathcal{D}_s = \{(\mathbf{x}_i^{(s)}, y_i^{(s)}) \in \mathcal{X}_s \times \mathcal{Y}_s\}_{i=1}^{N_s}$, $s = 1, 2, \dots, T$ where $\mathbf{x}_i^{(s)}, y_i^{(s)}$ and N_s denotes the input feature, label and sample size at timestamp t_s , respectively, and $\mathcal{X}_s, \mathcal{Y}_s$ denotes the input feature space and label space at timestamp t_s , respectively. The trained model will only be tested on some target domain *in the future*, i.e., \mathcal{D}_{T+1} where $t_{T+1} \geq t_T$. Our setting further assumes the existence of concept drift across different domains, i.e., the domain distribution is changing across time by following some patterns. For example, if we consider how personal income changes each year, we could find that the average income typically increases by some (varying) ratio every year due to the inflation. Similar patterns can also be found on the housing price and education cost, etc.

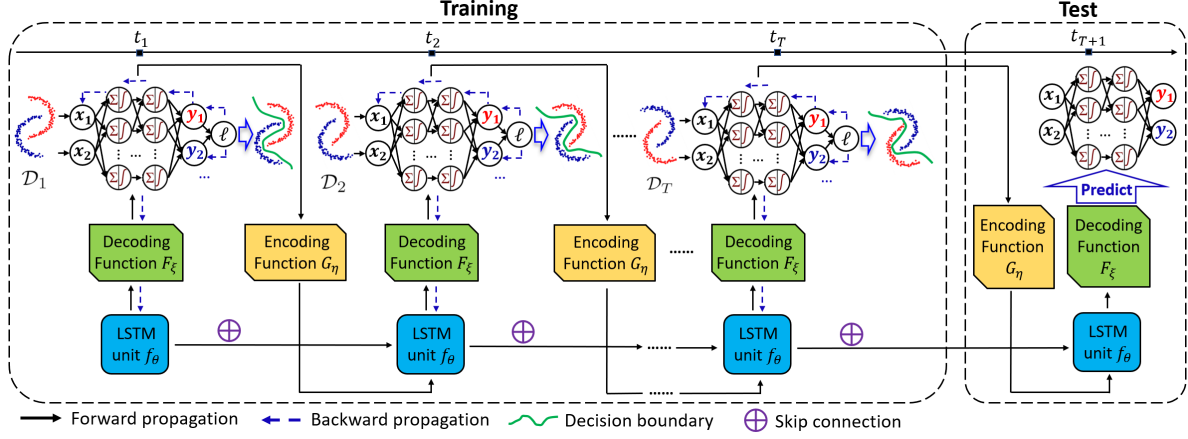


Figure 2: A high level overview of our DRAIN framework. Best viewed in color.

Our *goal* in this paper is to build a model that proactively captures the concept drift across time. Given labeled data from the source domains $\mathcal{D}_1, \mathcal{D}_2, \dots, \mathcal{D}_T$, we learn the mapping function $g_{\omega_s} : \mathcal{X}_s \rightarrow \mathcal{Y}_s$ on each domain \mathcal{D}_s , $s = 1, 2, \dots, T$ where ω_s denotes the function parameters at timestamp t_s , respectively, and then predict the dynamics across the parameters $\omega_1, \omega_2, \dots, \omega_T$. Finally, we predict the parameters ω_{T+1} for the mapping function $g_{\omega_{T+1}} : \mathcal{X}_{T+1} \rightarrow \mathcal{Y}_{T+1}$ on the unseen future domain. As shown in Figure 1, due to the temporal drift in data distribution, e.g. the input features such as Twitter user age distribution and number of tweets increase each year, the prediction model is expected to evolve accordingly, e.g. the magnitude of model parameter weights will decrease annually. Despite the necessity, handling the above problem is an open research area due to several existing challenges: 1) Difficulty in characterizing data distribution drift as well as how it influences the model. 2) Lack of expressiveness in automatically capturing the dynamics of how neural network evolves across time. 3) Theoretical guarantee on model's performance (e.g., generalization error, uncertainty) on future domains is hard to obtain due to the unknown and (potentially) complicated concept drift.

3.2 Temporal domain generalization with drift-aware dynamic neural network

In this section, we introduce how we address the challenges mentioned above. For the first challenge, we build a systematic Bayesian probability framework to represent the concept drift over the domains, which instantly differentiates our work from all existing methods in DG. For the second challenge, we propose modeling a neural network with changing parameters as a dynamic graph and achieving a temporal DG framework that can be trained end-to-end by graph generation techniques. We further improve the proposed method's generalization ability by introducing a skip connection module over different domains. Finally, to handle the last challenge, we explore theoretical guarantees of model performance under the challenging temporal DG setting and provide theoretical analyses of our proposed method, such as uncertainty and generalization error.

3.2.1 A probabilistic view of concept drift in temporal domain generalization.

To perform domain generalization over temporally indexed domains, we need to capture the concept drift within a given time interval. From a probabilistic point of view, for each domain \mathcal{D}_s , $s = 1, 2, \dots, T$, we can learn a neural network g_{ω_s} by maximizing the conditional probability $\Pr(\omega_s | \mathcal{D}_s)$, where ω_s denotes the status of model parameters at timestamp t_s . Due to the evolving distribution of \mathcal{D}_s , the conditional probability $\Pr(\omega_s | \mathcal{D}_s)$ will change over time accordingly. Our ultimate goal is to predict ω_{T+1} given all training data $\mathcal{D}_1, \mathcal{D}_2, \dots, \mathcal{D}_T$ ($\mathcal{D}_{1:T}$ for short), i.e., $\Pr(\omega_{T+1} | \mathcal{D}_{1:T})$. By the Law of total probability, we have

$$\Pr(\omega_{T+1} | \mathcal{D}_{1:T}) = \oint_{\Omega} \underbrace{\Pr(\omega_{T+1} | \omega_{1:T})}_{\text{inference}} \cdot \underbrace{\Pr(\omega_{1:T} | \mathcal{D}_{1:T})}_{\text{training}} d\omega_{1:T}. \quad (1)$$

The first term in the integral of Eq. 1 represents the inference phase, i.e., how we predict the status of the target neural network in the future (namely, ω_{T+1}) given all history statuses, while the second term denotes the training phase, i.e., how we leverage all source domains' training data $\mathcal{D}_{1:T}$ to obtain the status of the neural network on each source domain, namely $\omega_{1:T}$.

By chain rule of probability, we have

$$\begin{aligned} \Pr(\omega_{1:T} \mid \mathcal{D}_{1:T}) &= \prod_{s=1}^T \Pr(\omega_s \mid \omega_{1:s-1}, \mathcal{D}_{1:T}) \\ &= \Pr(\omega_1 \mid \mathcal{D}_1) \cdot \Pr(\omega_2 \mid \omega_1, \mathcal{D}_{1:2}) \cdots \Pr(\omega_T \mid \omega_{1:T-1}, \mathcal{D}_{1:T}) \end{aligned} \quad (2)$$

Notice that here we assume for each time point t_s , the model parameter ω_s only depends on the current and previous domains (namely, $\{\mathcal{D}_i : i \leq s\}$), and there is no access to future data (even unlabeled). Now we can break down the whole training process into $T - 1$ steps, where each step corresponds to learning the model parameter on the new domain conditional on parameter statuses from the history domains and training data, i.e.,

$$\Pr(\omega_{s+1} \mid \omega_{1:s}, \mathcal{D}_{1:s}, \mathcal{D}_{s+1}), \forall s < T \quad (3)$$

3.2.2 Neural network with dynamic parameters

Because the data distributions change temporally across data domains, the parameter ω_s in g_{ω_s} needs to be updated accordingly to address the temporal drift across the domains. In this work, we consider leveraging *dynamic graphs* to model the temporally evolving neural networks in order to retain maximal expressiveness across domains.

Intuitively, a neural network g_{ω} can be represented as an edge-weighted graph $G = (V, E, \psi)$, where each node $v \in V$ represents a neuron of g_{ω} while each edge $e \in E$ corresponds to a connection between two neurons in g_{ω} . Moreover, given a connection e between neuron u and v , i.e., $e = (u, v) \in E$, function $\psi : E \rightarrow \mathbb{R}$ denotes the weight parameter between these two neurons, i.e., $\psi(u, v) = w_{u,v}, \forall (u, v) \in E$. Essentially, $\omega = \psi(E) = \{w_{u,v} : (u, v) \in E\}$ is a set of parameter values indexed by all edges in E and ω represents the entire set of parameters for neural network g . Notice that we give a general definition of g_{ω} so that both shallow model (namely, linear model) and feed-forward network can be treated as special cases here. We aim to characterize the potential drift across domains by optimizing and updating the graph structure (i.e., edge weight) of g_{ω} . You et al. [36] have proven optimizing the graph structure of the neural network could have a smaller search space and a more smooth optimization procedure than exhaustively searching over all possible connectivity patterns.

We consider the case where the architecture or topology of neural network g_{ω} is given, i.e., V and E are fixed, while the parameter ω is changing constantly w.r.t time point t_s . In this sense, we can write $\omega_s = \psi(E|s)$ where $\psi(\cdot|s)$ (abbrev. ψ_s) depends only on time point t_s . Now the triplet $G = (V, E, \psi_s)$ defines a *dynamic graph* with evolving edge weights.

3.2.3 End-to-end learning of concept drift

Given history statuses of the neural network $\{\omega_{1:s}\}$ learned from $\{\mathcal{D}_{1:s}\}$, we aim at generalizing and extrapolating ω_{s+1} so that it produces good performance on the new domain \mathcal{D}_{s+1} in an end-to-end manner. In fact, by viewing the neural networks $\{\omega_{1:s}\}$ as dynamically evolving graphs, a natural choice is to characterize the latent graph distribution of $\{\omega_{1:s}\}$ by learning from its evolving trend. Consequently, ω 's can be directly sampled from the distribution for the prediction in future domains.

We characterize the latent distribution of $\{\omega_{1:s}\}$ as a sequential learning process based on a recurrent architecture, and each unit f_{θ} in the recurrent model is parameterized by θ to generate ω_s by accounting for previous $\{\omega_i : i < s\}$. Specifically, at each recurrent block (i.e., time step) t_s , f_{θ} produces two outputs (m_s, h_s) , where m_s is the current memory state and h_s is a latent probabilistic distribution (i.e., hidden output of f_{θ}) denoting the information carried from previous time steps. The latent probabilistic distribution h_t allows us to generate the dynamic graph ω_s by a decoding function $F_{\xi}(\cdot)$. Intuitively, different from existing works that train and regularize a neural network on single domain [19], here we focus on directly searching for distribution of networks with “good architectures”. Lastly, the sampled ω_s is encoded by a graph encoding function $G_{\eta}(\cdot)$, which then serves as the input of next recurrent block. Such a recurrent model is trained on a single domain \mathcal{D}_s to generate ω_s for prediction until convergence: $\min_{\theta, \xi, \eta} \sum_{i=1}^{N_s} \ell(g_{\omega_s}(\mathbf{x}_i^{(s)}), y_i^{(s)})$, where the choice of loss function $\ell(\cdot, \cdot)$ can depend on the actual task (i.e., cross-entropy for classification or mean squared error for regression). The optimal ω_s on domain \mathcal{D}_s will then be fed into the next domain \mathcal{D}_{s+1} . The optimal ω_s on domain \mathcal{D}_s will then be fed into the next domain \mathcal{D}_{s+1} along with the memory state m_s as input to guide the generation of ω_{s+1} .

3.2.4 Less forgetting and better generalization

During the training of recurrent models, it is also likely to encounter the performance degradation problem. Such a problem can be severe in temporal DG since a more complicated concept correlation exists between each domain. In addition, if the training procedure on each domain \mathcal{D}_s takes a large number of iterations to converge, we may also observe the forgetting phenomenon (i.e., the recurrent model f_{θ} will gradually focus on the current training domain and have less generalization capability for future domains). To alleviate such a phenomenon, we leverage a straightforward technique - skip connection to bridge the training on \mathcal{D}_s with previous domains $\mathcal{D}_{1:s-1}$. Specifically, we define the skip connection as:

$$\Phi(\omega_s, \{\omega_{s-\tau:s-1}\}) := \omega_s + \lambda \cdot \sum_{i=s-\tau}^{s-1} \omega_i \quad (4)$$

where the λ is a hyper-parameter for the regularization, and τ denotes the size of the *sliding window*. The skip connection could better enforce the generated neural network ω_s contains part of previous neural network information, and the implementation of the fixed-sized sliding window can better alleviate the potential drawback of the computational cost. We summarize the overall generative process in Appendix B due to the limited space.

3.3 Theoretical analysis

In this section, we provide theoretical analysis on our proposed framework's performance on target domain. Our analyses include uncertainty quantification and generalization error. Uncertainty characterizes the dispersion or error of an estimate due to the noise in measurements and the finite size of data sets [37], and smaller uncertainty means less margin of error over the model predictions. On the other hand, generalization error measures how accurately the model's prediction is on unseen data. Our analyses show that our proposed DRAIN achieves **both better prediction accuracy as well as smaller margin of error on target domain** compared with online and offline DG baselines.

First, we introduce two DG methods, namely online baseline and offline baseline as defined below:

Definition 1 (Online and Offline Baseline). Given time point t_{s+1} and domains $\mathcal{D}_1, \mathcal{D}_2, \dots, \mathcal{D}_{s+1}$, and model parameter state from previous time point, namely ω_s . Define online model \mathcal{M}_{on} as: $\omega_{s+1} = \text{argmax}_{\omega_{s+1}} \Pr(\omega_{s+1} | \omega_s, \mathcal{D}_{s+1})$ and offline model \mathcal{M}_{off} as $\omega_{s+1} = \text{argmax}_{\omega_{s+1}} \Pr(\omega_{s+1} | \mathcal{D}_{1:s+1})$.

Basically, offline method \mathcal{M}_{off} is time-oblivious and is trained using ERM over all source domains, while online method \mathcal{M}_{on} considers one-step finetuning over the model parameter on each new domain's dataset. Notice that \mathcal{M}_{on} is still not time-sensitive, since it cannot learn the concept drift across the sequential domains.

Assumption 1 (Prior on Concept Drift). *Suppose we consider a parameterized function $q_\theta(\cdot)$ to approximate the conditional probability $P(\omega_{t+1} | \omega_t)$, which is the unknown ground-truth concept drift of the model parameter. Without any training sample, we assume the prior over q_θ as a normal distribution with: $\mathbb{E}[q_{\theta_0}(\omega)] = \omega$, $\text{Var}(q_{\theta_0}(\omega)) = \sigma_{\theta_0}^2$, $\forall \omega \in \Omega$.*

Definition 2 (Predictive Distribution). Given training sample $\mathcal{D}_1, \mathcal{D}_2, \dots, \mathcal{D}_T$, and input feature from future domain, namely \mathbf{x}_{T+1} , the predictive distribution can be defined as

$$\begin{aligned} \Pr(\hat{y} | \mathbf{x}_{T+1}, \mathcal{D}_{1:T}) &= \oint_{\Omega} \Pr(\hat{y} | \mathbf{x}_{T+1}, \omega_{T+1}) \Pr(\omega_{T+1} | \mathcal{D}_{1:T}) d\omega_{T+1} \\ &= \oint_{\Omega} \Pr(\hat{y} | \mathbf{x}_{T+1}, \omega_{T+1}) \Pr(\omega_{T+1} | \omega_{1:T}) \Pr(\omega_{1:T} | \mathcal{D}_{1:T}) d\omega_{1:T+1} \end{aligned} \quad (5)$$

Our first theorem below shows that by capturing the concept drift over the sequential domains, our proposed method always achieves the smallest uncertainty in prediction on the future domain.

Theorem 1 (Uncertainty Quantification). *Given training sample $\mathcal{D}_1, \mathcal{D}_2, \dots, \mathcal{D}_T$, we have the following inequality over each method's predictive uncertainty, i.e., the variance of predictive distribution as defined in Eq. 5: $\text{Var}(\mathcal{M}_{\text{ours}}) < \text{Var}(\mathcal{M}_{\text{on}}) \leq \text{Var}(\mathcal{M}_{\text{off}})$.*

Our second theorem shows that, besides uncertainty, our proposed method can also achieve smallest generalization error thanks to learning the concept drift.

Definition 3. Given predictive distribution in Eq. 5, as well as ground-truth label y_{T+1} from the future domain, define the predictive or generalization error as $\text{err} := \ell(\mathbb{E}[P(\hat{y} | \mathbf{x}_{T+1}, \mathcal{D}_{1:T})], y_{T+1})$.

Theorem 2 (Generalization Error). *We have the following inequality over each method's predictive error defined above: $\text{err}(\mathcal{M}_{\text{ours}}) < \text{err}(\mathcal{M}_{\text{on}}) < \text{err}(\mathcal{M}_{\text{off}})$.*

All proofs can be found in appendix due to limited space.

4 Experiment

In this section, we present the performance of DRAIN against other state-of-the-art approaches with both quantitative and qualitative analysis; additional experiment settings and results (e.g., hyperparameter setting and scalability analysis) are demonstrated in the appendix.

4.1 Experiment setting

Datasets. We compare with the following classification datasets: Rotated Moons (2-Moons), Rotated MNIST (Rot-MNIST), Online News Popularity (ONP), Electrical Demand (Elec2), and Shuttle; and the following regression datasets:

Table 1: Performance comparison of all methods in terms of misclassification error (in %) for classification tasks and mean absolute error (MAE) for regression tasks. "-" denotes the method could not converge on the specific dataset.

Model	Classification (in %)					Regression	
	2-Moons	Rot-MNIST	ONP	Shuttle	Elec2	House	Appliance
Offline	22.4 \pm 4.6	35.3 \pm 3.4	33.8 \pm 0.6	0.77 \pm 0.1	23.0 \pm 3.1	11.0 \pm 0.36	10.2 \pm 1.1
LastDomain	14.9 \pm 0.9	32.7 \pm 2.1	36.0 \pm 0.2	0.91 \pm 0.18	25.8 \pm 0.6	10.3 \pm 0.16	9.1 \pm 0.7
IncFinetune	16.7 \pm 3.4	28.5 \pm 1.2	34.0 \pm 0.3	0.83 \pm 0.07	27.3 \pm 4.2	9.7 \pm 0.01	8.9 \pm 0.5
CDOT	9.3 \pm 1.0	30.3 \pm 2.4	34.1 \pm 0.0	0.94 \pm 0.17	17.8 \pm 0.6	-	-
CIDA	10.8 \pm 1.6	27.1 \pm 1.5	34.7 \pm 0.6	-	14.1 \pm 0.2	9.7 \pm 0.06	8.7 \pm 0.2
GI	6.5 \pm 1.2	25.6 \pm 1.7	36.4 \pm 0.8	0.29 \pm 0.05	16.9 \pm 0.7	9.6 \pm 0.02	8.2 \pm 0.6
Ours	5.6 \pm 1.1	21.6 \pm 1.4	38.3 \pm 1.2	0.31 \pm 0.05	12.7 \pm 0.8	9.3 \pm 0.14	6.4 \pm 0.4

House prices dataset (House), Appliances energy prediction dataset (Appliance). The first two datasets are synthetic, where the rotation angle is used as a proxy for time. The remaining datasets are real-world datasets with temporally evolving characteristics. Dataset details can be found at Appendix A.1.

Comparison Methods. We adopt three sets of comparison methods: **practical baselines** that do not consider the concept drift, including 1). *Offline* that treats all source domains as a single domain, 2). *LastDomain* that employs the last training domain for model training, and 3). *IncFinetune* that uses temporal information as an auxiliary feature to sequentially train on each training domain. **Continuous domain adaptation methods** that focus only on DA, including 1). *CDOT* [15] that transports most recent labeled examples to the future, and 2). *CIDA* [16] that specifically tackles the continuous DA problem; and one **temporal domain generalization method**: *GI* [19].

All experiments are repeated 10 times for each comparison method, and we report the average results and the standard deviation in the following quantitative analysis. More detailed description of each comparison method and the parameter setting can be found in Appendix A.2 and A.3, respectively.

4.2 Quantitative analysis

We firstly illustrate the performance of our proposed method against other comparison methods. The experiments are conducted in both classification and regression tasks with the domain generalization setting, i.e., models are trained on the training domains and deployed on the unseen testing domain. The results are depicted in Table 1.

As can be clearly seen from the table, DRAIN consistently achieves competitive results across all datasets with only one exception. Specifically, DRAIN excels the second-best approach in 2-Moons, Rot-MNIST, and Elec2 by on average 15%, and the performance of DRAIN has little margin between the state-of-the-art model GI in the Shuttle dataset. The only exception exists in the ONP dataset, where the Offline method achieves the best result and all state-of-the-art methods cannot generalize well on unseen testing domains since the ONP dataset does not exhibit a strong concept drift. Additionally, all time-oblivious baselines perform rather unsatisfactorily since they are not capable of handling the concept drift of the data distribution. Both CDOT and CIDA can generate better results than time-oblivious baselines, yet their generalization ability on the unseen domains is still limited as the maintained time-invariant representation in both methods cannot address the concept drift without any data in the testing domain. As the only method that addresses the temporal domain generalization problem, GI imposes a gradient regularization with a non-parametric activation function to handle the concept drift, which relies too much on the task-specific heuristic. In contrast, DRAIN proposes to sequentially model each domain in an end-to-end manner, which could address the concept drift more inherently.

4.3 Qualitative analysis

We compare different methods qualitatively by visualizing the decision boundary on the 2-Moons dataset. As shown in Figure 3a - 3c, we demonstrate the decision boundary predicted by DRAIN at \mathcal{D}_2 , \mathcal{D}_4 , \mathcal{D}_6 training domains on the 2-Moons dataset, and the final predicted decision boundary on the unseen testing domain \mathcal{D}_9 (Figure 3d). As can be seen from the figure, DRAIN can successfully characterize the concept drift of the data distribution by sequentially modeling the $\{\mathcal{D}_T\}$, and the learned decision boundary could rotate correctly along time.

We further visualize the decision boundary learned by other comparison methods in Figure 4a - 4f. Firstly, the left subfigure in Figure 4a shows the decision boundary learned by the Offline method on the concatenated training domains $\{\mathcal{D}_{1:T}\}$, and the learned decision boundary overfits the training data and shows poor performance when generalizing on the unseen testing domain (the right subfigure of 4a). The other two time-oblivious baselines: LastDomain (Figure 4b) and IncFinetune (Figure 4c) can generate better decision boundaries than the Offline method, but they still cannot achieve satisfying results on the unseen domain since they lack the capability of characterizing the concept drift

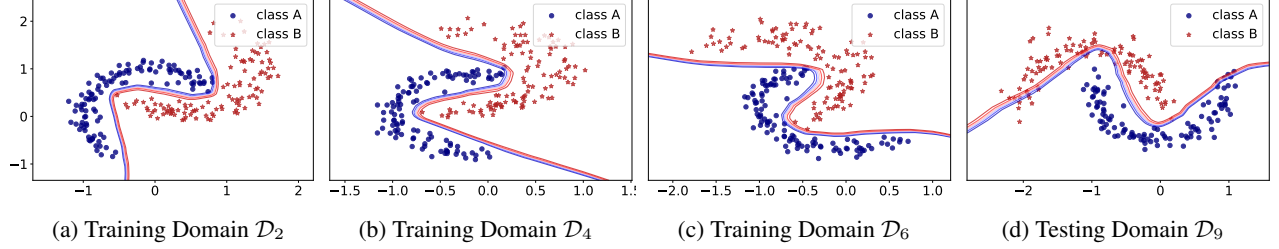


Figure 3: The visualization of decision boundary of DRAIN (blue dots and red stars represent different data classes). As the distribution of data points are consistently changing, as shown in Figure 3a - 3c, DRAIN can effectively characterize such a temporal drift and predict accurate decision boundaries on the unseen testing domain in Figure 3d.

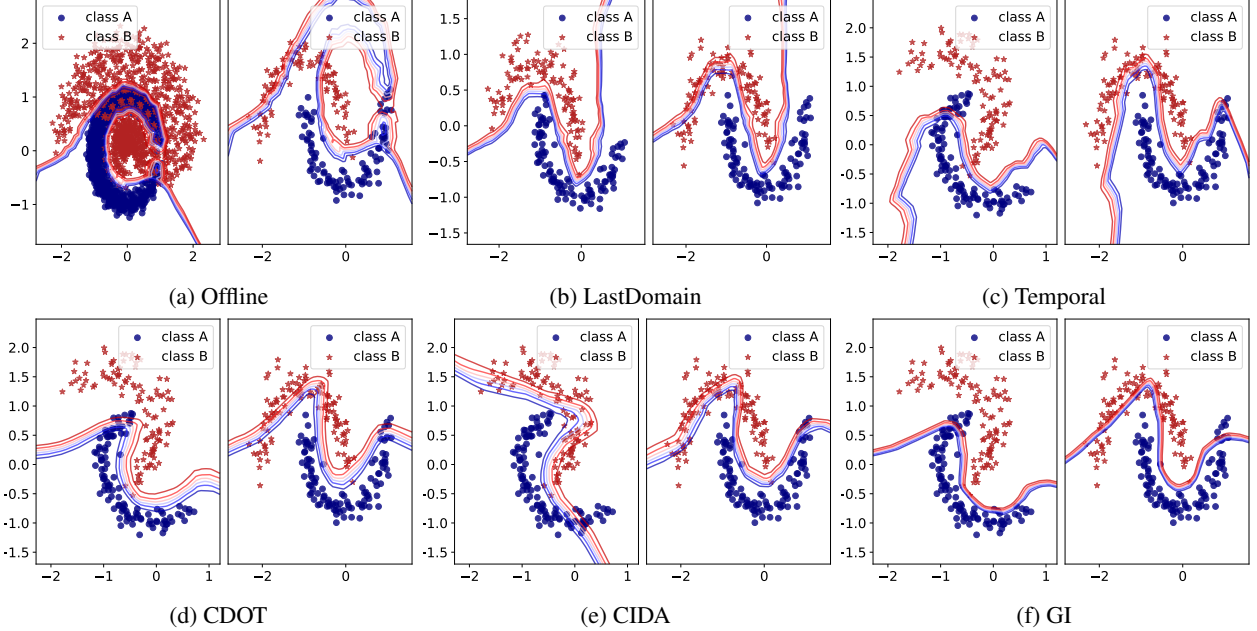


Figure 4: **Visualization of decision boundary** (blue dots and red stars represent different data classes), where the right subfigure of comparison methods Figure 4a - 4f demonstrate the decision boundary predicted for the test domain \mathcal{D}_{T+1} , the left subfigure in Figure 4a shows the decision boundary learned from the all data points in the concatenated training domain ($[\mathcal{D}_1, \dots, \mathcal{D}_T]$), the left subfigure in Figure 4b shows the decision boundary learned from all samples in the last training domain \mathcal{D}_T , and the left subfigures in Figure 4c - 4f show the decision boundary learned on \mathcal{D}_4 .

of the data distribution. Furthermore, as the current state-of-the-art continuous domain adaptation methods, CDOT transports the most recent labeled data points in \mathcal{D}_T to the future, which makes the learned decision boundary almost temporal-invariant (Figure 4d) and cannot generalize well in the scenario of domain generalization. CIDA utilizes the adversarial training technique to solve the domain adaptation, yet the predicted decision boundary in Figure 4e is less stable than other state-of-the-art methods due to its model complexity. Lastly, even though GI is the only method proposed to tackle the temporal domain generalization problem, the produced decision boundaries, as shown in both the training domain and testing domain (Figure 4f), are still less accurate than our proposed method, since they heavily utilize heuristics to regularize the gradient.

4.4 Sensitivity analysis

We conduct sensitivity analysis on the depth of the neural network g_{ω_s} for the proposed method. As shown in Figure 5, the optimal number of hidden layers for g_{ω_s} is 2 and 1 on 2-Moons and Electric dataset, respectively. The curve on both datasets has an inverse "U" shape, meaning that too few layers may limit the general expressiveness of our model, while too many layers could potentially hurt the generalization ability due to overfitting.

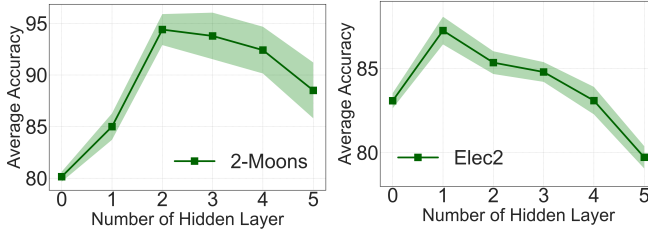


Figure 5: Sensitivity analysis on the number of layers of generated neural network by DRAIN.

Table 2: Ablation study. Comparison of performance between our method and two alternatives across two datasets for classification tasks and one datasets for regression tasks.

Ablation	2-Moons	Rot-MNIST	House
✗ RNN	22.4 ± 4.6	35.3 ± 3.4	11.0 ± 0.36
✗ Skip.C	7.1 ± 1.3	23.3 ± 3.6	9.7 ± 0.13
Ours.	5.6 ± 1.1	21.6 ± 1.4	9.3 ± 0.14

4.5 Ablation study

We further conduct ablation study on three datasets (2-Moons, Elec2, and House) to evaluate the effect of different components in DRAIN, and the results are exhibited in Table 2. The ablative experiments are conducted based on each of the essential components in our architecture. Specifically, we remove the sequential learning model in DRAIN, and the resulted ablated model **✗ RNN** corresponds to the IncFinetune baseline model. We also independently remove the skip connection module to let the sequential learning model uniformly acquire information from all previous domains, and the resulting model is named **✗ Skip.C**.

As shown in the table, yet each component can effectively contribute to the overall model performance, modeling the temporal correlation between all domains by a sequential model can provide a rather larger performance gain. In addition, removing the skip connection module in the sequential learning model would make DRAIN hard to capture the long range temporal dependency among domains since long range domain information could potentially be forgotten during the model learning.

5 Conclusion

We tackle the problem of domain generalization over temporally indexed domains by proposing a drift-aware dynamic neural network framework. We build a Bayesian framework to model the concept drift and then model a neural network as a dynamic graph and attain a framework that can be trained in an end-to-end manner by graph generation techniques. We also provide formal theoretical analyses of our proposed method, such as uncertainty and generalization error, and extensive empirical results to demonstrate the efficacy and efficiency of our method.

References

- [1] Shai Ben-David, John Blitzer, Koby Crammer, Alex Kulesza, Fernando Pereira, and Jennifer Wortman Vaughan. A theory of learning from different domains. *Machine learning*, 79(1):151–175, 2010.
- [2] Yaroslav Ganin, Evgeniya Ustinova, Hana Ajakan, Pascal Germain, Hugo Larochelle, François Laviolette, Mario Marchand, and Victor Lempitsky. Domain-adversarial training of neural networks. *The journal of machine learning research*, 17(1):2096–2030, 2016.
- [3] Eric Tzeng, Judy Hoffman, Kate Saenko, and Trevor Darrell. Adversarial discriminative domain adaptation. In *Proceedings of the IEEE conference on computer vision and pattern recognition*, pages 7167–7176, 2017.
- [4] Shiv Shankar, Vihari Piratla, Soumen Chakrabarti, Siddhartha Chaudhuri, Preethi Jyothi, and Sunita Sarawagi. Generalizing across domains via cross-gradient training. *arXiv preprint arXiv:1804.10745*, 2018.
- [5] Martin Arjovsky, Léon Bottou, Ishaan Gulrajani, and David Lopez-Paz. Invariant risk minimization. *arXiv preprint arXiv:1907.02893*, 2019.
- [6] Qi Dou, Daniel Coelho de Castro, Konstantinos Kamnitsas, and Ben Glocker. Domain generalization via model-agnostic learning of semantic features. *Advances in Neural Information Processing Systems*, 32, 2019.
- [7] Yann LeCun, Léon Bottou, Yoshua Bengio, and Patrick Haffner. Gradient-based learning applied to document recognition. *Proceedings of the IEEE*, 86(11):2278–2324, 1998.

- [8] Yuval Netzer, Tao Wang, Adam Coates, Alessandro Bissacco, Bo Wu, and Andrew Y Ng. Reading digits in natural images with unsupervised feature learning. 2011.
- [9] Alex Krizhevsky, Ilya Sutskever, and Geoffrey E Hinton. Imagenet classification with deep convolutional neural networks. *Advances in neural information processing systems*, 25, 2012.
- [10] Tsung-Yi Lin, Michael Maire, Serge Belongie, James Hays, Pietro Perona, Deva Ramanan, Piotr Dollár, and C Lawrence Zitnick. Microsoft coco: Common objects in context. In *European conference on computer vision*, pages 740–755. Springer, 2014.
- [11] Krikamol Muandet, David Balduzzi, and Bernhard Schölkopf. Domain generalization via invariant feature representation. In *International Conference on Machine Learning*, pages 10–18. PMLR, 2013.
- [12] Saeid Motiian, Marco Piccirilli, Donald A Adjeroh, and Gianfranco Doretto. Unified deep supervised domain adaptation and generalization. In *Proceedings of the IEEE international conference on computer vision*, pages 5715–5725, 2017.
- [13] Yogesh Balaji, Swami Sankaranarayanan, and Rama Chellappa. Metareg: Towards domain generalization using meta-regularization. *Advances in neural information processing systems*, 31, 2018.
- [14] Judy Hoffman, Trevor Darrell, and Kate Saenko. Continuous manifold based adaptation for evolving visual domains. In *Proceedings of the IEEE Conference on Computer Vision and Pattern Recognition*, pages 867–874, 2014.
- [15] Guillermo Ortiz-Jimenez, Mireille El Gheche, Effrosyni Simou, Hermina Petric Maretic, and Pascal Frossard. Cdot: Continuous domain adaptation using optimal transport. *arXiv preprint arXiv:1909.11448*, 2019.
- [16] Hao Wang, Hao He, and Dina Katabi. Continuously indexed domain adaptation. *arXiv preprint arXiv:2007.01807*, 2020.
- [17] Da Li, Yongxin Yang, Yi-Zhe Song, and Timothy Hospedales. Sequential learning for domain generalization. In *European Conference on Computer Vision*, pages 603–619. Springer, 2020.
- [18] Chelsea Finn, Pieter Abbeel, and Sergey Levine. Model-agnostic meta-learning for fast adaptation of deep networks. In *International conference on machine learning*, pages 1126–1135. PMLR, 2017.
- [19] Anshul Nasery, Soumyadeep Thakur, Vihari Piratla, Abir De, and Sunita Sarawagi. Training for the future: A simple gradient interpolation loss to generalize along time. *Advances in Neural Information Processing Systems*, 34, 2021.
- [20] Alexey Dosovitskiy, Lucas Beyer, Alexander Kolesnikov, Dirk Weissenborn, Xiaohua Zhai, Thomas Unterthiner, Mostafa Dehghani, Matthias Minderer, Georg Heigold, Sylvain Gelly, et al. An image is worth 16x16 words: Transformers for image recognition at scale. *arXiv preprint arXiv:2010.11929*, 2020.
- [21] Fengxiang He and Dacheng Tao. Recent advances in deep learning theory. *arXiv preprint arXiv:2012.10931*, 2020.
- [22] Mei Wang and Weihong Deng. Deep visual domain adaptation: A survey. *Neurocomputing*, 312:135–153, 2018.
- [23] Atsutoshi Kumagai and Tomoharu Iwata. Learning future classifiers without additional data. In *Thirtieth AAAI Conference on Artificial Intelligence*, 2016.
- [24] Atsutoshi Kumagai and Tomoharu Iwata. Learning non-linear dynamics of decision boundaries for maintaining classification performance. In *Proceedings of the AAAI Conference on Artificial Intelligence*, volume 31, 2017.
- [25] Massimiliano Mancini, Samuel Rota Bulo, Barbara Caputo, and Elisa Ricci. Adagraph: Unifying predictive and continuous domain adaptation through graphs. In *Proceedings of the IEEE/CVF Conference on Computer Vision and Pattern Recognition*, pages 6568–6577, 2019.
- [26] Da Li, Yongxin Yang, Yi-Zhe Song, and Timothy M Hospedales. Deeper, broader and artier domain generalization. In *Proceedings of the IEEE international conference on computer vision*, pages 5542–5550, 2017.
- [27] Jindong Wang, Cuiling Lan, Chang Liu, Yidong Ouyang, Wenjun Zeng, and Tao Qin. Generalizing to unseen domains: A survey on domain generalization. *arXiv preprint arXiv:2103.03097*, 2021.
- [28] Josh Tobin, Rachel Fong, Alex Ray, Jonas Schneider, Wojciech Zaremba, and Pieter Abbeel. Domain randomization for transferring deep neural networks from simulation to the real world. In *2017 IEEE/RSJ international conference on intelligent robots and systems (IROS)*, pages 23–30. IEEE, 2017.
- [29] Jonathan Tremblay, Aayush Prakash, David Acuna, Mark Brophy, Varun Jampani, Cem Anil, Thang To, Eric Cameracci, Shaad Boochoon, and Stan Birchfield. Training deep networks with synthetic data: Bridging the reality gap by domain randomization. In *Proceedings of the IEEE conference on computer vision and pattern recognition workshops*, pages 969–977, 2018.

- [30] Alexander H Liu, Yen-Cheng Liu, Yu-Ying Yeh, and Yu-Chiang Frank Wang. A unified feature disentangler for multi-domain image translation and manipulation. *Advances in neural information processing systems*, 31, 2018.
- [31] Fengchun Qiao, Long Zhao, and Xi Peng. Learning to learn single domain generalization. In *Proceedings of the IEEE/CVF Conference on Computer Vision and Pattern Recognition*, pages 12556–12565, 2020.
- [32] Rui Gong, Wen Li, Yuhua Chen, and Luc Van Gool. Dlow: Domain flow for adaptation and generalization. In *Proceedings of the IEEE/CVF conference on computer vision and pattern recognition*, pages 2477–2486, 2019.
- [33] Wen Li, Zheng Xu, Dong Xu, Dengxin Dai, and Luc Van Gool. Domain generalization and adaptation using low rank exemplar svms. *IEEE transactions on pattern analysis and machine intelligence*, 40(5):1114–1127, 2017.
- [34] Massimiliano Mancini, Samuel Rota Bulo, Barbara Caputo, and Elisa Ricci. Best sources forward: domain generalization through source-specific nets. In *2018 25th IEEE international conference on image processing (ICIP)*, pages 1353–1357. IEEE, 2018.
- [35] Zeyi Huang, Haohan Wang, Eric P Xing, and Dong Huang. Self-challenging improves cross-domain generalization. In *European Conference on Computer Vision*, pages 124–140. Springer, 2020.
- [36] Jiaxuan You, Jure Leskovec, Kaiming He, and Saining Xie. Graph structure of neural networks. In *International Conference on Machine Learning*, pages 10881–10891. PMLR, 2020.
- [37] Christopher M Bishop and Nasser M Nasrabadi. *Pattern recognition and machine learning*, volume 4. Springer, 2006.
- [38] Li Deng. The mnist database of handwritten digit images for machine learning research [best of the web]. *IEEE signal processing magazine*, 29(6):141–142, 2012.
- [39] Kelwin Fernandes, Pedro Vinagre, and Paulo Cortez. A proactive intelligent decision support system for predicting the popularity of online news. In *Portuguese conference on artificial intelligence*, pages 535–546. Springer, 2015.
- [40] Luis M Candanedo, Véronique Feldheim, and Dominique Deramaix. Data driven prediction models of energy use of appliances in a low-energy house. *Energy and buildings*, 140:81–97, 2017.

Appendix

A Experimental Details

A.1 Dataset Details

- **Rotated 2 Moons:** This is a variant of the 2-entangled moons dataset, with a lower moon and an upper moon labeled 0 and 1 respectively. Each moon consists of 100 instances, and 10 domains are obtained by sampling 200 data points from the 2-Moons distribution, and rotating them counter-clockwise in units of 18° . Domains 0 to 8 (both inclusive) are our training domains, and domain 9 is for testing.
- **Rotated MNIST:** This is an adaptation of the popular MNIST digit dataset [38], where the task is to classify a digit from 0 to 9 given an image of the digit. We generate 5 domains by rotating the images in steps of 15 degrees. To generate the i -th domain, we sample 1,000 images from the MNIST dataset and rotate them counter-clockwise by $15 \times i$ degrees. We take the first four domains as train domains and the fifth domain as test.
- **Online News Popularity:** This dataset [39] summarizes a heterogeneous set of features about articles published by Mashable in a period of two years. The goal is to predict the number of shares in social networks (popularity). We split the dataset by time into 6 domains and use the first 5 for training.
- **Shuttle:** This dataset provides about 58,000 data points for space shuttles in flight. The task is multiclass classification with a heavy class imbalance. The dataset was divided into 8 domains based on the time points associated with points, with times between 30-70 being the train domains and 70 -80 being the test domain.
- **Electrical Demand** This contains information about the demand of electricity in a particular province. The task is, again binary classification, to predict if the demand of electricity in each period (of 30 mins) was higher or lower than the average demand over the last day. We consider two weeks to be one time domain, and train on 29 domains while testing on domain 30.
- **House Prices Dataset:** This dataset has housing price data from 2013-2019. This is a regression task to predict the price of a house given the features. We treat each year as a separate domain, but also give information about the exact date of purchase to the models. We take data from the year 2019 to be test data and prior data as training.
- **Appliances Energy Prediction:** This dataset [40] is used to create regression models of appliances energy use in a low energy building. The data set is at 10 min for about 4.5 months in 2016, and we treat each half month as a single domain, resulting in 9 domains in total. The first 8 domains are used for training and the last one is for testing.

A.2 Details of Comparison Methods

- **Practical Baseline.** 1). *Offline*: this is a time-oblivious model that is trained using ERM on all the source domains. 2). *LastDomain*: this is a time-oblivious model that is trained using ERM on the last source domains. 3). *IncFinetune*: we bias the training towards more recent data by applying the Baseline method described above on the first time point and then, fine-tuning with a reduced learning rate on the subsequent time points in sequential manner. This baseline corresponds to the online model we defined in Definition 1.
- **Continuous Domain Adaptation Methods.** 1). *CDOT*: this model transports most recent labeled examples \mathcal{D}^T to the future using a learned coupling from past data, and trains a classifier on them.. 2). *CIDA*: this method is representative of typical domain erasure methods applied to continuous domain adaptation problems. 3). *Adagraph*: This method makes the batch norm parameters time-sensitive and smooths them using a given kernel.
- **Temporal Domain Generalization Method.** 1). *GI*: this method proposes a training algorithm to encourage a model to learn functions which can extrapolate well to the near future by supervising the first order Taylor expansion of the learnt function.

A.3 Parameter Setting

We use Adam optimizer for all our experiments, and the learning rate for all datasets are uniformly set to be $1e - 4$. All experiments are conducted on a 64-bit machine with 4-core Intel Xeon W-2123 @ 3.60GHz, 32GB memory and NVIDIA Quadro RTX 5000. We set hyperparameters for each comparison method with respect to the recommendation in their original paper, and we specify the architecture as well as other details for each dataset's experiments as follows.

- **2-Moons.** The number of layers in the LSTM is set to be 10, and the network architecture of g_{ω_t} consists of 2 hidden layers, with a dimension of 50 each. We use ReLU layer after each hidden layer and a Sigmoid layer after the output layer. The learning rate is set to be $1e - 4$.
- **Rot-MNIST.** The number of layers in the LSTM is set to be 15, and the network architecture of g_{ω_t} consists of 3 hidden layers with bias terms, and the dimensions of each layer are 512, 128, and 10. We use ReLU layer after each hidden layer and a Sigmoid layer after the output layer. The learning rate is set to be $1e - 4$.

Table 3: Comparison of training time (seconds) between our method and two baselines across two datasets for classification tasks and one datasets for regression tasks.

Model	2-Moons	Elec2	Appliance
CIDA	45.2 ± 0.87	154.3 ± 2.1	287.5 ± 2.6
GI	19.3 ± 0.43	136.4 ± 1.9	189.3 ± 2.1
Ours.	15.4 ± 0.37	99.2 ± 1.3	170.3 ± 1.8

- **ONP.** The number of layers in the LSTM is set to be 10, and the network architecture of g_{ω_t} consists of 2 hidden layers with bias terms, and the dimensions of each layer are 20. We use ReLU layer after each hidden layer and a Sigmoid layer after the output layer. The learning rate is set to be $1e-4$.
- **Shuttle.** The number of layers in the LSTM is set to be 5, and the network architecture of g_{ω_t} consists of 3 hidden layers with bias terms, and the dimensions of each layer are 128. We use ReLU layer after each hidden layer and a Sigmoid layer after the output layer. The learning rate is set to be $5e-5$.
- **Elec2.** The number of layers in the LSTM is set to be 10, and the network architecture of g_{ω_t} consists of 2 hidden layers with bias terms, and the dimensions of each layer are 128. We use ReLU layer after each hidden layer and a Sigmoid layer after the output layer. The learning rate is set to be $5e-5$.
- **House.** The number of layers in the LSTM is set to be 10, and the network architecture of g_{ω_t} consists of 2 hidden layers with bias terms, and the dimensions of each layer are 128. We use ReLU layer after each hidden layer and no activation layer after the output layer. The learning rate is set to be $1e-5$.
- **Appliance.** The number of layers in the LSTM is set to be 10, and the network architecture of g_{ω_t} consists of 2 hidden layers with bias terms, and the dimensions of each layer are 128. We use ReLU layer after each hidden layer and no activation layer after the output layer. The learning rate is set to be $1e-5$.

A.4 Training Time Analysis

We further conduct the model scalability analysis by comparing the running time of our proposed method with two other state-of-the-art baselines: GI and CIDA on three datasets (i.e., 2-Moons, Elec2, and Appliance). As shown in Table 3, our proposed method can generally achieve the shortest training time among the three methods. However, we notice that GI is relatively slower in the total running time due to the model pretraining and finetuning step, and the low efficiency in CIDA is due to the expensive computation cost for training GAN. Compared to these approaches, DRAIN only consists of one sequential learning model to address the data distribution drift in the end-to-end manner, which could achieve generally better performance while attaining its efficiency.

B Overall generation process

$$\begin{aligned}
 a_1 &= 0, m_1 = G_0(z), z \sim \mathcal{N}(0, 1) \\
 a_1 &= G_\eta(\omega_1), \omega_1 \sim F_\xi(h_1), (m_1, h_1) = f_\theta(m_0, a_0) \\
 &\dots \\
 a_1 &= G_\eta(\omega_1), \omega_1 \sim G_o(h_1), (m_1, h_1) = f_\theta(m_1, a_1) \\
 a_2 &= G_\eta(\omega_2), \omega_2 = \Phi(\omega_2, \{\omega_1\}), \omega_2 = F_\xi(h_1), (m_2, h_2) = f_\theta(m_1, a_1) \\
 &\dots \\
 a_2 &= G_\eta(\omega_2), \omega_2 = \Phi(\omega_2, \{\omega_1\}), \omega_2 = F_\xi(h_1), (m_2, h_2) = f_\theta(m_2, a_2) \\
 &\dots \\
 a_t &= G_\eta(\omega_t), \omega_t = \Phi(\omega_t, \{\omega_{t-\tau:t-1}\}), \omega_t = F_\xi(h_1), (m_t, h_t) = f_\theta(m_t, a_t),
 \end{aligned}$$

where each a_t denotes the input of f_θ . In this work, we utilize LSTM as the recurrent architecture, and f_θ becomes a single LSTM unit. To initialize the whole generative process, we take a random noise z as input for the first domain \mathcal{D}_1 , which is drawn from a standard Gaussian distribution. The initial memory state m_1 is also transformed from z by an initial encoding function $G_0(\cdot)$.

C Theory Proof

In this section, we provide the formal proof for Theorem 1 and Theorem 2 in our main context.

C.1 Proof for Theorem 1

Proof. By definition of the predictive distribution,

$$\begin{aligned} P(\hat{y}|\mathbf{x}_{T+1}, \mathcal{D}_{1:T}) &= \oint_{\Omega} P(\hat{y}|\mathbf{x}_{T+1}, \omega_{T+1}) P(\omega_{T+1}|\mathcal{D}_{1:T}) d\omega_{T+1} \\ &= \oint_{\Omega} P(\hat{y}|\mathbf{x}_{T+1}, \omega_{T+1}) P(\omega_{T+1}|\omega_{1:T}) P(\omega_{1:T}|\mathcal{D}_{1:T}) d\omega_{1:T+1} \end{aligned} \quad (6)$$

Our goal is to prove that the variance of this predictive distribution for our proposed method, online baseline and offline baseline follows the inequality as in Theorem 1.

Ours v.s. Online Baseline

Here we prove that $\text{Var}(\mathcal{M}_{\text{ours}}) < \text{Var}(\mathcal{M}_{\text{on}})$.

Notice that the first term on the right hand side of Eq. 6, namely $P(\hat{y}|\mathbf{x}_{T+1}, \omega_{T+1})$, corresponds to deployment of the model with parameter ω_{T+1} on the future domain \mathcal{D}_{T+1} , hence the variance of $P(\hat{y}|\mathbf{x}_{T+1}, \omega_{T+1})$ only depends on the noise or randomness coming from \mathbf{x}_{T+1} as long as ω_{T+1} is given. In other words, the uncertainty coming from $P(\hat{y}|\mathbf{x}_{T+1}, \omega_{T+1})$ can be cancelled for both methods since we are considering the same set of domains. Now the problem reduces to prove that the variance of the second and third terms on the right hand side of Eq. 6 for our model is smaller than those for the online baseline.

By Bayesian statistics, we know that

$$P(\omega_{1:T}|\mathcal{D}_{1:T}) = \int_{\Theta} P(\omega_1|\mathcal{D}_1) \cdot P(\omega_2|\omega_1, \mathcal{D}_2, \theta_0) \cdot P(\theta_1|\omega_1, \omega_2, \theta_0) \cdot P(\omega_3|\omega_2, \mathcal{D}_3, \theta_1) \cdot P(\theta_2|\omega_2, \omega_3, \theta_1) \cdots P(\omega_T|\omega_{T-1}, \mathcal{D}_T, \theta_{T-2}) \cdot P(\theta_{T-1}|\omega_{T-1}, \omega_T, \theta_{T-2}) d\theta_{0:T-1} \quad (7)$$

where θ is the parameter of the parameterized function to approximate the ground-truth drift of ω , as defined in Assumption 1. For example, $P(\omega_1|\mathcal{D}_1)$ denotes that we train the model on the very first domain and $P(\omega_2|\omega_1, \mathcal{D}_2, \theta_0)$ denotes that we continue to train the model on the second domain but with initialization of ω_2 as $q_{\theta_0}(\omega_1)$ where ω_1 is learned from the previous domain and q_{θ_0} is trying to capture the conditional probability or drift between ω_2 and ω_1 , i.e., $P(\omega_2|\omega_1)$. In our Bayesian framework, we treat q_{θ} as a learnable function (e.g., LSTM unit in our proposed method) and we use subscript of θ to differentiate the status of θ after the training on each domain. In other words, q_{θ} will be updated after the training on each domain (at least for our method). Notice that θ_0 always denotes the prior distribution as in Assumption 1.

By Bayes' rule, we have:

$$P(\omega_{t+1}|\omega_t, \mathcal{D}_{t+1}, \theta_{t-1}) \propto \underbrace{P(q_{\theta_{t-1}}(\omega_t))}_{\text{prior on } \omega_{t+1}} \cdot \underbrace{P(\mathcal{D}_{t+1}|\omega_{t+1})}_{\text{likelihood}} \quad (8)$$

where $P(q_{\theta_{t-1}}(\omega_t))$ can be regarded as the prior of ω_{t+1} because as we mentioned $q_{\theta_{t-1}}$ denotes the initialization of ω_{t+1} before we train the model on domain \mathcal{D}_{t+1} , and $P(\mathcal{D}_{t+1}|\omega_{t+1})$ corresponds to the likelihood of training ω_{t+1} on \mathcal{D}_{t+1} .

In addition,

$$\begin{aligned} P(\theta_t|\omega_t, \omega_{t+1}, \theta_{t-1}) &\propto P(\theta_{t-1}) \cdot P(\omega_t, \omega_{t+1}|\theta_t) \\ &\propto P(\theta_{t-2}) \cdot P(\omega_{t-1}, \omega_t|\theta_{t-1}) \cdot P(\omega_t, \omega_{t+1}|\theta_t) \\ &\cdots \\ &\propto \underbrace{P(\theta_0)}_{\text{prior on } \theta} \cdot \underbrace{\prod_{i=1}^t P(\omega_i, \omega_{i+1}|\theta_i)}_{\text{likelihood}} \end{aligned} \quad (9)$$

for any $t = 1, 2, 3, \dots, T-1$. In the equation above, this time the prior is over parameter θ and ω_i, ω_{i+1} can be regarded as the "training data" for θ_i .

For the online baseline, since it only keeps one-step finetuning of the model and does not learn how ω_t evolves, the θ_t for the online baseline is always equal to the prior, i.e. $\theta_t = \theta_0$. In other words, $P(q_{\theta_{t-1}}(\omega_t)) = P(q_{\theta_0}(\omega_t))$ and $P(\theta_t|\omega_t, \omega_{t+1}, \theta_{t-1}) = P(\theta_0)$, $\forall t$ for the online baseline.

Since we follow the standard routine and assume all distributions are Gaussian, by Bayesian Theorem, we know that the posterior distribution always has variance smaller than the prior distribution, hence we know that

$$Var(\theta_t|\omega_t, \omega_{t+1}, \theta_{t-1}) < Var(\theta_0) \quad (10)$$

which proves that our method has smaller variance in terms of Eq. 9. On the other hand, since the second term on the right hand side of Eq. 8 is the same for both methods, and for the first term $P(q_{\theta_{t-1}}(\omega_t))$, by our Assumption 1 we know that for baseline $Pr(q_{\theta_{t-1}}(\omega_t)) = Pr(q_{\theta_0}(\omega_t))$ so the variance is basically σ_{θ_0} . For our method, after each training step across a new domain our θ will get updated and achieve smaller variance (because of posterior variance of Gaussian) so we also prove that our method has smaller variance in terms of Eq. 8. Two parts combined prove that our method has smaller variance in the third term of Eq. 6, namely $P(\omega_{1:T}|\mathcal{D}_{1:T})$.

The last step is to compare the variance from the second term in Eq. 6, namely $P(\omega_{T+1}|\omega_{1:T})$. For online baseline, basically it uses the parameter from the last training domain, i.e., ω_T as the final model on the future domain, i.e.,

$$P(\omega_{T+1}|\omega_{1:T}) = P(q_{\theta_0}(\omega_T)) \quad (11)$$

On the other hand, for our method,

$$P(\omega_{T+1}|\omega_{1:T}) = P(q_{\theta_{T-1}}(\omega_T)) \quad (12)$$

which has smaller variance due to the posterior variance of Gaussian.

All together we finish the proof for $Var(\mathcal{M}_{\text{ours}}) < Var(\mathcal{M}_{\text{on}})$.

Online Baseline v.s. Offline Baseline

This case is simpler to prove. Again, the first term on the right hand side of Eq 6, namely $P(\hat{y}|\mathbf{x}_{T+1}, \omega_{T+1})$ can be cancelled in this case. Moreover, the second term, namely $P(\omega_{T+1}|\omega_{1:T})$ has the same variance for both baselines, i.e.,

$$Var(P(\omega_{T+1}|\omega_{1:T})) = Var(P(q_{\theta_0}(\omega_T))) = \sigma_{\theta_0} \quad (13)$$

This makes sense since two baselines do not learn the drift and the uncertainty in predicting ω_{T+1} based on ω_T is always the same as the prior distribution of θ_0 .

Hence, it suffices to compare the uncertainty of the last term of Eq. 6, namely $P(\omega_{1:T}|\mathcal{D}_{1:T})$. Recall that

$$\begin{aligned} \mathcal{M}_{\text{on}} : \quad \omega_{t+1} &= \underset{\omega_{t+1}}{\text{argmax}} P(\omega_{t+1}|\omega_t, \mathcal{D}_{t+1}) \\ \mathcal{M}_{\text{off}} : \quad \omega_{t+1} &= \underset{\omega_{t+1}}{\text{argmax}} P(\omega_{t+1}|\mathcal{D}_{1:t+1}) \end{aligned} \quad (14)$$

For offline baseline, we are using all dataset so far, namely $\mathcal{D}_{1:t+1}$ to train the model while the online baseline only uses \mathcal{D}_{t+1} . Since in this paper, we are considering domain generalization with temporal concept drift, i.e., for each $i \neq j$ we have $\mathcal{D}_i \neq \mathcal{D}_j$ (otherwise we merge them), the randomness of $\bigcup_{i=1}^{t+1} \mathcal{D}_i$ is at least as large as that of \mathcal{D}_{t+1} alone, i.e., $Var(\bigcup_{i=1}^{t+1} \mathcal{D}_i) \geq Var(\mathcal{D}_{t+1})$. Again, by Bayes' rule, we can finish the proof. \square

C.2 Proof of Theorem 2

Proof. Recall that

$$err := \ell(\mathbb{E}[P(\hat{y}|\mathbf{x}_{T+1}, \mathcal{D}_{1:T})], y_{T+1}) \quad (15)$$

First denote the ground-truth θ for the parameterized function q_θ as q_{θ^*} . The general idea of the proof below is to show that our method can achieve θ that is closer to the ground-truth θ^* , i.e., learning the dynamics of $\{\omega_t\}_{t=1}^T$ more accurately.

Notice that

$$\mathbb{E}[P(\omega_{T+1}|\omega_{1:T})] = \mathbb{E}[q_\theta(\omega_T)] \quad (16)$$

By Assumption 1, we know that by learning the conditional probability $P(\omega_{t+1}|\omega_t)$ our method can update θ of q_θ . Assume that after training on the first T domains, our model can achieve error as defined by:

$$\mathbb{E}[\|q_{\theta_{T-1}}(\omega_T) - q_{\theta^*}(\omega_T)\|_2] < \mathbb{E}[\|q_{\theta_0}(\omega_T) - q_{\theta^*}(\omega_T)\|_2] \quad (17)$$

where the left hand side denotes the expected error between the predicted ω_{T+1} and the ground-truth for our method while the right hand side denotes that for the online baseline.

With some mild assumptions over the neural network, i.e., Lipschitz continuity of the neural network w.r.t the parameter, we can measure that the prediction error for our model is smaller than that of online baseline.

On the other hand, for the comparison between two baselines, we consider a simpler case where the drift of ω_t is monotonic but our proof can be generalized to other cases easily.

As can be shown,

$$\begin{aligned} \text{Online baseline: } & \mathbb{E}[P(\omega_{T+1}|\omega_{1:T})] = \mathbb{E}[q_{\theta_0}(\omega_T)] = \omega_T \\ \text{Offline baseline: } & \mathbb{E}[P(\omega_{T+1}|\omega_{1:T})] = \mathbb{E}[q_{\theta_0}(\bar{\omega})] = \mathbb{E}[P(\omega|\mathcal{D}_{1:T})] \end{aligned} \quad (18)$$

If we denote a distance function over the domains, as d , we assume that

$$d(\mathcal{D}_{t+1}, \mathcal{D}_{T+1}) < d(\mathcal{D}_t, \mathcal{D}_{T+1}) \quad (19)$$

By the monotonic assumption, the distribution of each $\mathcal{D}_{1:T}$ is changing along a certain direction. Hence, among them \mathcal{D}_T has the distribution most close to that of \mathcal{D}_{T+1} . In other words, the online baseline finetunes the model so its ω_T is leaning towards the last domain while the offline baseline is using the averaged domains to train the model, which finishes the proof. \square